Supporting Information

Synthesis and Polymorphism of Mixed Aluminium-Gallium Oxides

Daniel S. Cook, Joseph E. Hooper, Daniel M. Dawson, Janet M. Fisher, David Thompsett, Sharon E. Ashbrook and Richard I. Walton

Contents:

S1. Additional Data for $Ga_{5-x}Al_xO_7(OH)$

Table S1: Refined lattice parameters in the system $Ga_{5-x}Al_xO_7(OH)$, ($0 \leq x \leq 1.5$).

	Lattice parameters			
Material	***a* / Å**	***c* / Å**	**Volume / Å^3**	**Reference**
$Ga_5O_7(OH)$	5.82107(8)	9.0662(2)	266.05	[1]
$Ga_{4.5}Al_{0.5}O_7(OH)$	5.8037(3)	9.0386(8)	263.66(11)	This work
$Ga_{4.0}Al_{1.0}O_7(OH)$	5.7855(4)	9.0262(10)	261.65(9)	This work
$Ga_{3.5}Al_{1.5}O_7(OH)$	5.7605(5)	9.0121(14)	258.99(14)	This work
$Al_5O_7(OH)$	5.576	8.768	236.09	[2]

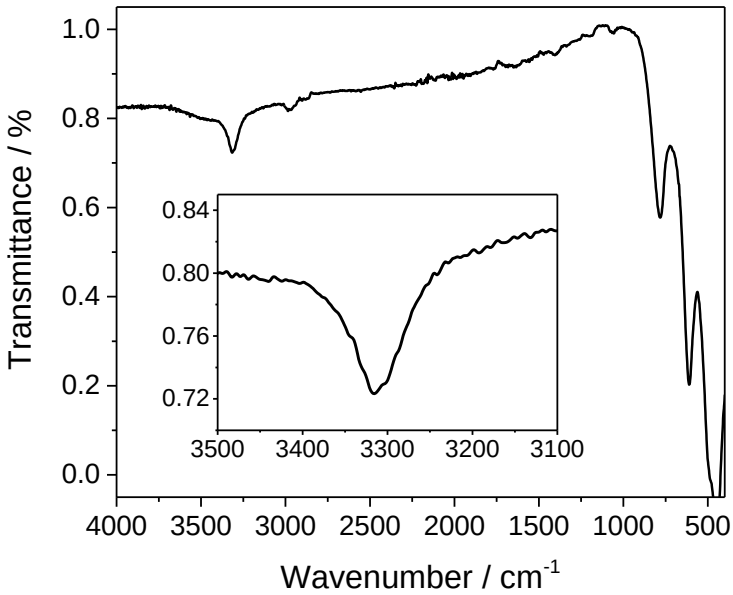

Figure S1: *IR spectrum of $Ga_{3.5}Al_{1.5}O_7(OH)$ showing a stretching mode at 3300 cm^{-1} and Ga-O-H bending mode at 850 cm^{-1}.*

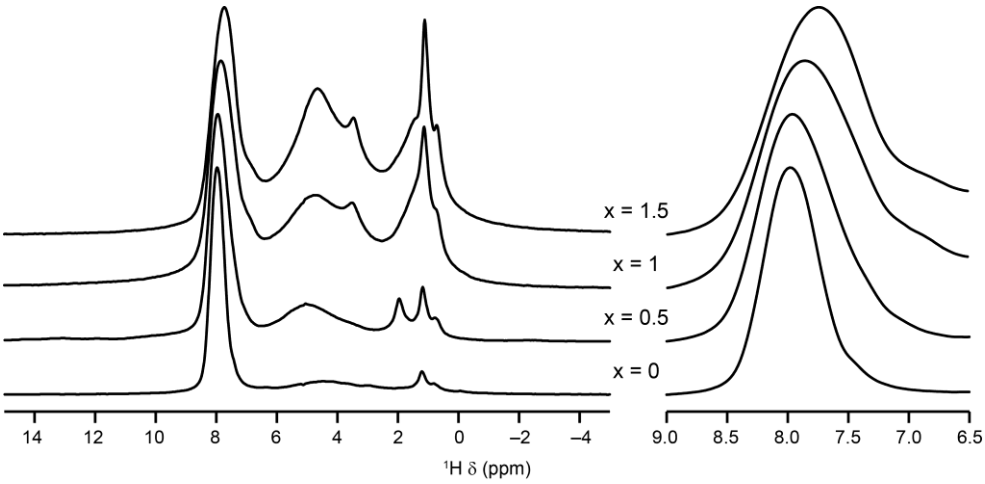

Figure S2: *^{1}H (14.1 T, 55 kHz MAS) NMR spectra of $Ga_{5-x}Al_xO_7(OH)$. The signals below 6 ppm are attributed to residual solvent from the synthesis and atmospheric water, both adsorbed on the surfaces of the crystallites.*

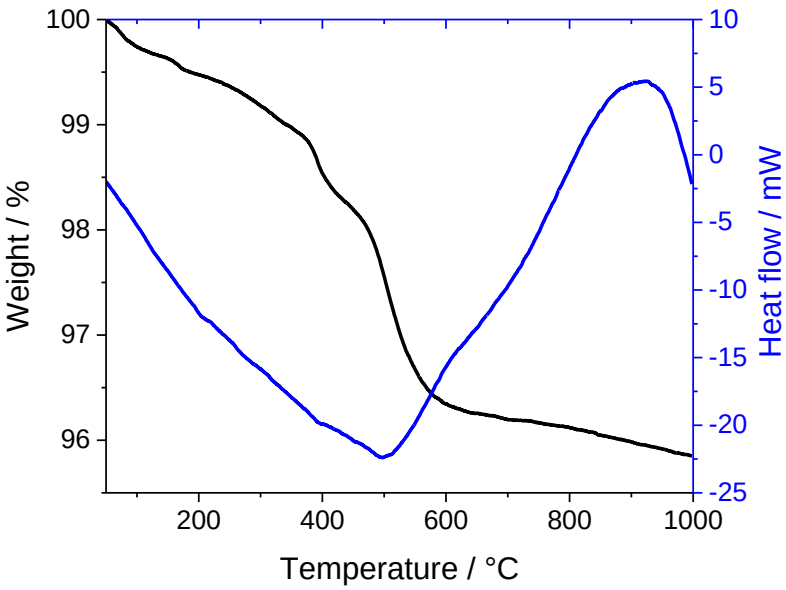

Figure S3: *TGA/DSC-trace of $Ga_{3.5}Al_{1.5}O_7(OH)$.*

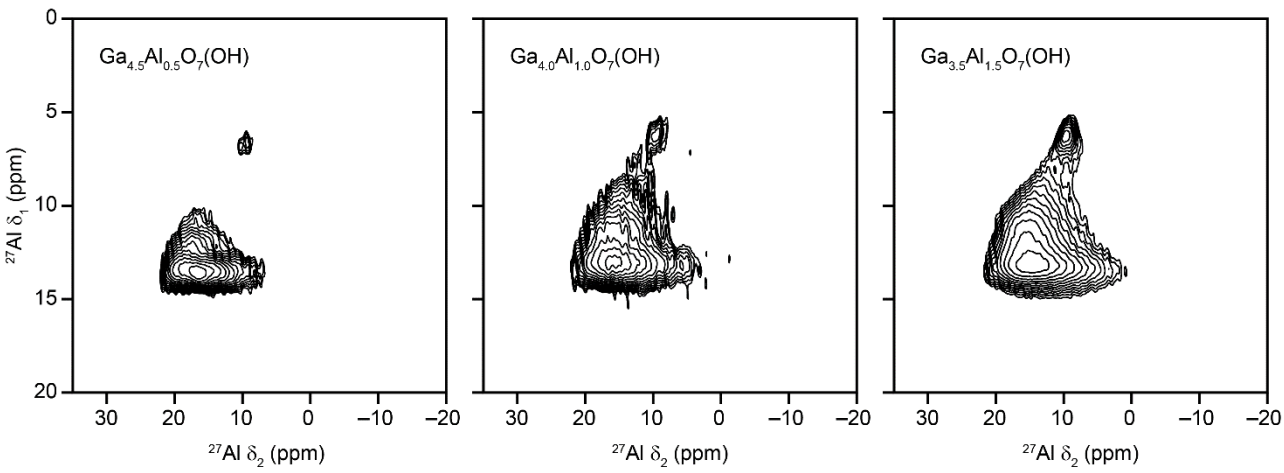

Figure S4: *^{27}Al (14.1 T, 20 kHz) MQMAS NMR spectra of $Ga_{4.5}Al_{0.5}O_7(OH)$, $Ga_{4.0}Al_{1.0}O_7(OH)$ and $Ga_{3.5}Al_{1.5}O_7(OH)$, shown after shearing and referencing.[3] Sum projections onto the isotropic dimension are shown in Figure 4(d) of the main text.*

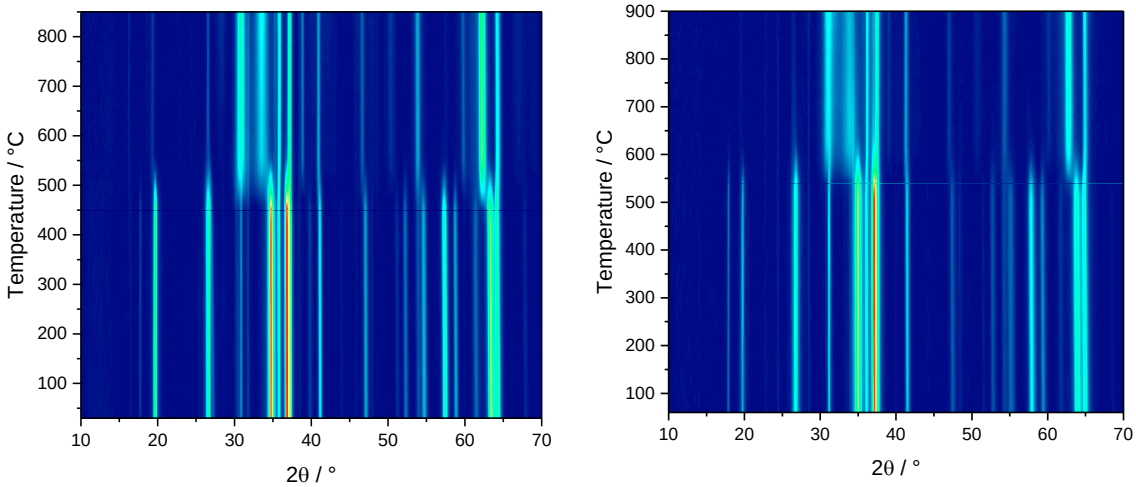

Figure S5: *Thermodiffractometry of (left) $Ga_{4.5}Al_{0.5}O_7(OH)$, and (right) $Ga_4AlO_7(OH)$, which decomposes at a higher temperature, showing collapse into ε-$Ga_{2-x}Al_xO_3$ and κ-$Ga_{2-x}Al_xO_3$.*

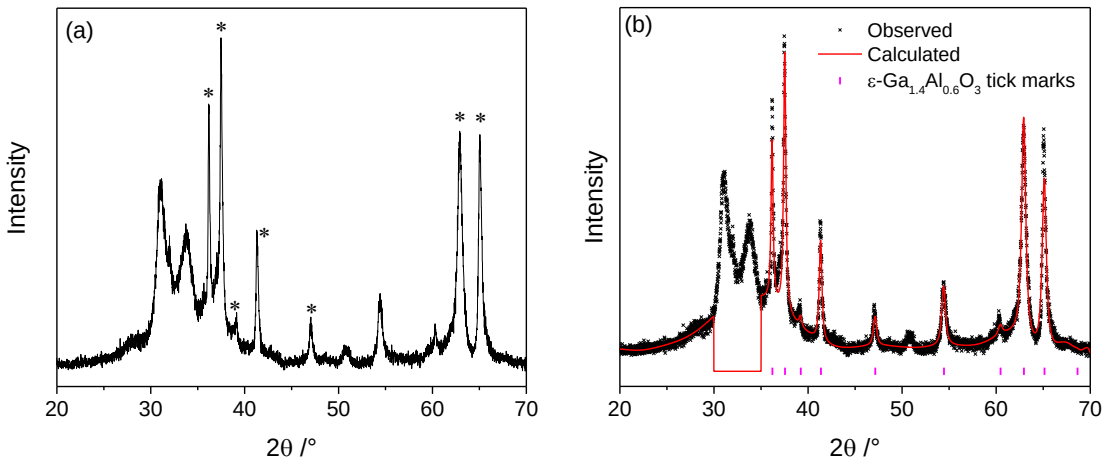

Figure S6: *(a) Measured PXRD data for $Ga_{3.5}Al_{1.5}O_7(OH)$ after heating to 900 °C forming ε- and κ-$Ga_{2-x}Al_xO_3$ phases (*) denotes ε phase, (b) Pawley refinement to measured data for ε-$Ga_{2-x}Al_xO_3$, the region between 30 and 35 °2θ was not calculated due to overlap with peaks of the κ-phase.*

S2. Further Details of DFT Calculations

The calculation of NMR parameters was carried out using the CASTEP density functional theory (DFT) code (version 18.1),[4] employing the gauge-including projector augmented wave (GIPAW) approach[5] to reconstruct the all-electron wavefunction in the presence of a magnetic field. Calculations were performed using the GGA PBE functional,[6] with dispersion corrections provided by the scheme of Tkatchenko and Scheffler.[7] Ultrasoft pseudopotentials were used with the inclusion of ZORA scalar relativistic effects. A planewave energy cutoff of 60 Ry (~816 eV) was used, and integrals over the first Brillouin zone were performed using a Monkhorst-Pack grid[8] with a *k*-point spacing of 0.03 or 0.04 2π $Å^{-1}$. Optimisation of atomic coordinates and unit cell parameters was carried out prior to the calculation of NMR parameters. Calculations were performed on a computing cluster at the University of St Andrews, consisting of 90 32-core Intel Broadwell nodes, Infiniband FDR interconnect and a 300 TB GPFS distributed filesystem. Typical calculation times were between 3 and 10 h (geometry optimisation) and ~1 h (NMR parameters), using 48 cores.

The quadrupolar coupling constant, $C_Q = eQV_{ZZ}/h$, and the asymmetry parameter, $\eta_Q = (V_{XX} - V_{YY})/V_{ZZ}$, are obtained directly from the principal components of the electric field gradient tensor, **V**. Q is the nuclear quadrupole moment,[9] for which values of 146.6 and 107 mb were used for ^{27}Al and ^{71}Ga, respectively. The on-the-fly (OTF) pseudopotential generated by default for Ga:

Ga 3|2.0|10|12|13|40:41:32(qc=6)

was shown to underestimate C_Q and so a modified pseudopotential:

Ga 3|1.6|14|16|19|30U:40:31U:41:32(qc=7)

was used to explicitly describe more of the polarisable core electrons. Isotropic shieldings, σ_{iso}, were obtained from the trace of the absolute shielding tensor, $\boldsymbol{\sigma}$, and isotropic chemical shifts, δ_{iso}, were given by $\delta_{iso} = -(\sigma_{ref} - \sigma_{iso}) / m$. The values of the reference shielding, σ_{ref}, and scaling factor, m, were determined, respectively, from the y-intercept and gradient of a plot of calculated σ_{iso} against experimental δ_{iso} for a series of reference species. For ^{27}Al, the reference points were the octahedral and tetrahedral sites in θ-Al_2O_3, whereas for ^{71}Ga, the octahedral and tetrahedral sites of β-Ga_2O_3 (isostructural with θ-Al_2O_3) were used. This approach yielded values of σ_{ref} and m of 562.4 ppm and 1.07 for ^{27}Al and 1740 ppm and 1.01 (≈1.00) for ^{71}Ga.

Structural models for $Ga_{5-x}Al_xO_7(OH)$

The unit cell of $Ga_5O_7(OH)$, shown in Figure S7, contains two formula units, giving a total of six octahedral Ga1, two octahedral Ga2 and two tetrahedral Ga3. The Ga1 sites fall into two "layers" per cell, with Ga2 and Ga3 occupying sites between these layers. For this work, we considered models for Al substitution onto all three sites with one or two Al atoms per cell ($Ga_{5-x}Al_xO_7(OH)$ with x = 0.5 or 1.0). For a single Al atom, substitution was considered onto sites 1, 2 and 3 (models **1**, **2** and **3**, respectively). When considering two Al atoms, their relative positions must be taken into account: models **4a** and **4b** consider the substitution of two Al1 in the same layer (*i.e.*, creating an Al(OH)Al bridge) and in separate layers (creating two Al(OH)Ga bridges), respectively. Models **5** and **6** consider Al1 + Al2 and Al1 + Al3, respectively. Figure S8 shows these models. The energy of each model is reported relative to the model with the lowest energy of each composition, and these relative energies are reported in Table S3 in eV per unit cell and in kJ mol^{-1} on a per formula unit and per cation basis (where the latter allows more ready comparison with the models for β-Ga_2O_3). Note that the substitution of Al2 or Al3 is disfavoured by roughly the same amount in both compositions, regardless of the number of Al1 present, such that models of composition $Ga_{3.5}Al_{1.5}O_7(OH)$ were not investigated. The calculated ^{27}Al and ^{71}Ga NMR parameters for all models considered are given in Table S4.

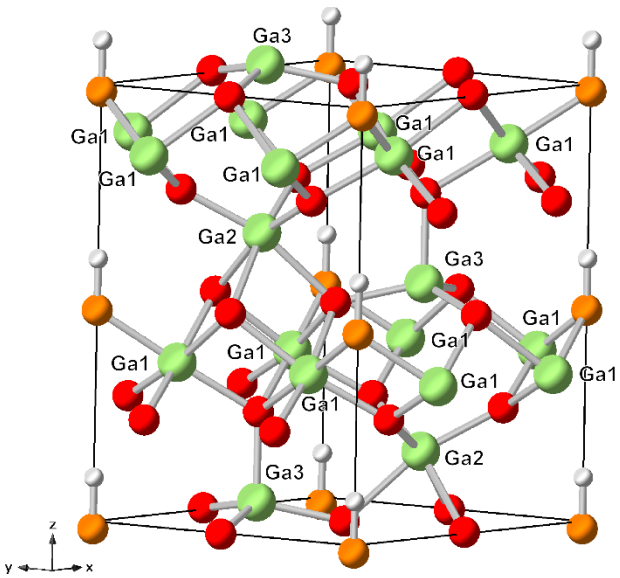

Figure S7: *The structure of $Ga_5O_7(OH)$. Atoms are coloured with Ga = green, O^{2-} = red, $O(H)^-$ = orange, H = grey.*

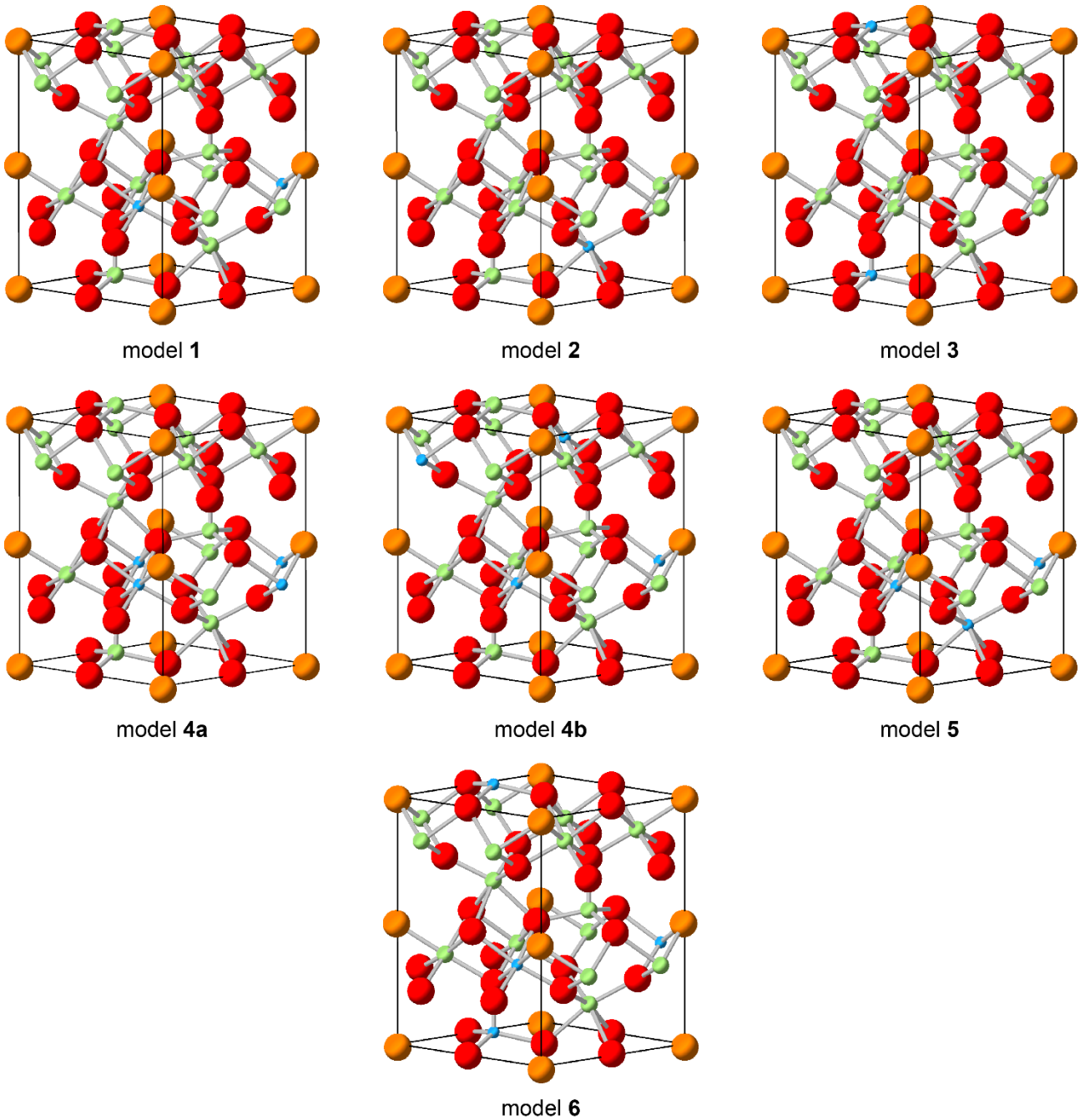

Figure S8: *The structural models for $Ga_{5-x}Al_xO_7(OH)$. Atoms are coloured with Al = blue, Ga = green, O = red, O(H) = orange. H atoms are omitted.*

Table S2: Computed relative energies of the models of $Ga_{5-x}Al_xO_7(OH)$ (after geometry optimisation). Energies are reported in eV per unit cell and kJ mol^{-1} on a per formula unit and per cation basis.

Model	Relative energy / eV per cell	Relative energy / kJ per mole $Ga_{5-x}Al_xO_7(OH)$	Relative energy / kJ per mole cations
1	0	0	0
2	0.215	10.4	2.08
3	0.519	25.0	5.00
4a	0.060	2.88	0.577
4b	0	0	0
5	0.276	13.3	2.66
6	0.556	26.8	5.36

Table S3: Computed ^{27}Al and ^{71}Ga NMR parameters for the structural models of $Ga_{5-x}Al_xO_7(OH)$. Note that, upon Al substitution, the symmetry is lost and all ten cation sites are distinct: the labels 11-16 correspond to site 1 in the parent structure, 21 and 22 to site 2 and 31 and 32 to site 3.

Model	Atom	δ_{iso} (ppm)	$\lvert C_Q \rvert$ / MHz	η_Q
$Ga_5O_7(OH)$	Ga1	83.2	9.9	0.71
	Ga2	14.6	4.3	0.03
	Ga3	135.7	11.3	0.02
1	Al11	27.5	3.7	0.69
	Ga12	82.5	12.5	0.56
	Ga13	82.1	12.6	0.55
	Ga14	87.7	10.2	0.62
	Ga15	87.5	9.7	0.69
	Ga16	87.6	9.7	0.68
	Ga21	17.6	4.4	0.67
	Ga22	19.3	4.2	0.28
	Ga31	144.9	10.9	0.17
	Ga32	135.2	11.6	0.27
2	Al21	17.1	2.0	0.07
	Ga11	83.4	8.4	0.96

	Ga12	83.5	8.3	0.94
	Ga13	83.6	8.4	0.96
	Ga14	87.7	9.6	0.70
	Ga15	87.7	9.5	0.71
	Ga16	87.6	9.6	0.70
	Ga22	19.2	2.7	0.03
	Ga31	127.1	12.0	0.01
	Ga32	137.6	13.7	0.01
3	Al31	66.7	4.7	0.01
	Ga11	85.3	11.4	0.62
	Ga12	85.4	11.4	0.62
	Ga13	85.4	11.3	0.63
	Ga14	80.7	8.7	0.90
	Ga15	80.7	8.7	0.90
	Ga16	80.7	8.6	0.91
	Ga21	13.4	5.6	0.01
	Ga22	21.2	4.8	0.03
	Ga32	138.4	11.9	0.01
4a	Al11	25.3	5.0	0.53
	Al12	25.3	5.0	0.52
	Ga13	81.3	15.0	0.41
	Ga14	93.9	10.0	0.63
	Ga15	93.6	10.1	0.62
	Ga16	93.1	10.1	0.58
	Ga21	20.6	4.4	0.79
	Ga22	22.9	4.0	0.16
	Ga31	153.9	11.0	0.18
	Ga31	135.7	11.5	0.26
4b	Al11	27.9	3.4	0.79
	Al14	27.8	3.4	0.79
	Ga12	85.1	12.5	0.47
	Ga13	85.2	12.5	0.47
	Ga15	85.2	12.5	0.48
	Ga16	85.2	12.5	0.48

	Ga21	20.9	4.3	0.96
	Ga22	21.9	4.4	0.96
	Ga31	143.2	11.2	0.35
	Ga32	143.9	11.0	0.35
5	Al11	26.9	2.8	0.93
	Al21	17.1	2.0	0.59
	Ga12	82.9	10.9	0.79
	Ga13	82.8	10.9	0.78
	Ga14	92.6	10.1	0.62
	Ga15	92.0	9.5	0.69
	Ga16	91.9	9.5	0.68
	Ga22	21.3	2.0	0.32
	Ga31	136.4	12.3	0.14
	Ga32	136.7	13.6	0.22
6	Al11	26.9	4.0	0.72
	Al31	67.2	4.6	0.17
	Ga12	84.2	13.9	0.5
	Ga13	84.1	13.9	0.5
	Ga14	85.3	8.8	0.86
	Ga15	84.1	8.5	0.87
	Ga16	84.2	8.5	0.86
	Ga21	15.6	5.7	0.64
	Ga22	24.9	4.6	0.11
	Ga32	136.7	12.2	0.22

Models for β-Ga_2O_3

The unit cell of β-Ga_2O_3, shown in Figure S9, contains four formula units, giving a total of four tetrahedral Ga1 and four octahedral Ga2. Structure description. For β-Ga_2O_3, two models were considered, with a single Al atom substituted onto the octahedral or tetrahedral sites (models **β1** and **β2**, respectively, shown in Figure S9). The relative energies of each model are reported in Table S5 in eV per unit cell and in kJ mol^{-1} on a per formula unit and per cation basis, where the latter allows more ready comparison with the models for $Ga_{5-x}Al_xO_7(OH)$. The calculated ^{27}Al and ^{71}Ga NMR parameters for all models considered are given in Table S6.

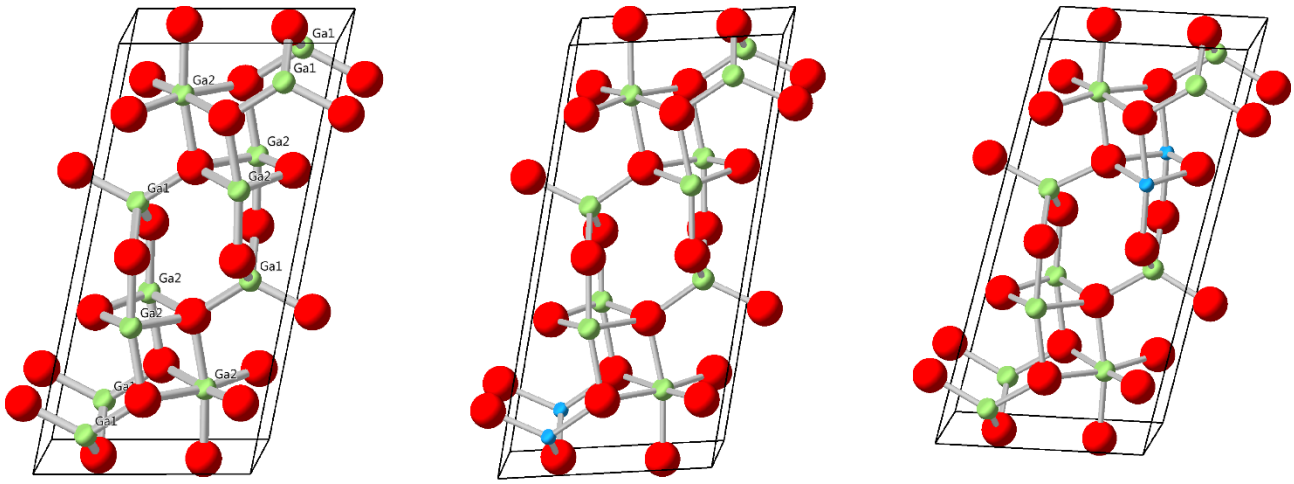

β-Ga_2O_3 model **β1** model **β2**

Figure S9: *Structures of β-Ga_2O_3 and the two structural models for β-$Ga_{2-x}Al_xO_3$. Atoms are coloured with Al = blue, Ga = green, O = red.*

Table S4: Computed relative energies of the models of β-$Ga_{2-x}Al_xO_3$ (after geometry optimisation). Energies are reported in eV per unit cell and kJ mol^{-1} on a per formula unit and per cation basis.

Model	Relative energy / eV per cell	Relative energy / kJ per mole β-$Ga_{2-x}Al_xO_3$	Relative energy / kJ per mole cations
β1	0.169	4.07	2.03
β2	0	0	0

Table S5: Computed ^{27}Al and ^{71}Ga NMR parameters for the structural models of β-$Ga_{2-x}Al_xO_3$. Note that, upon Al substitution, the symmetry is lost and all eight cation sites are distinct: the labels 11-14 correspond to site 1 in the parent structure and 21 and 24 to site 2.

Model	Atom	δ_{iso} (ppm)	$\lvert C_Q \rvert$ / MHz	η_Q
β-Ga_2O_3	Ga1	214.5	11.5	0.05
	Ga2	41.6	8.4	0.27
β1	Al11	75.8	7.7	0.34
	Ga12	217.5	10.5	0.27
	Ga13	227.3	12.3	0.14
	Ga14	221.4	10.7	0.18
	Ga21	43.3	7.9	0.28

	Ga22	39.1	4.0	0.72
	Ga23	44.3	6.5	0.19
	Ga24	36.8	10.9	0.06
β2	Al21	21.0	5.4	0.62
	Ga11	217.7	9.8	0.26
	Ga12	216.6	10.0	0.29
	Ga13	219.2	12.2	0.30
	Ga14	211.9	14.2	0.11
	Ga22	46.1	6.3	0.28
	Ga23	49.1	8.0	0.13
	Ga24	45.2	9.2	0.10

S3. Additional Data for γ-$Ga_{2-x}Al_xO_3$

Table S6: EDX measurements from scanning electron microscopy averaged from 6 different areas of γ-$Ga_{2-x}Al_xO_3$ materials.

Sample	Average Ga At%	Average Al At%
γ-$Ga_{1.4}Al_{0.6}O_3$	68	32
γ-$Ga_1Al_1O_3$	53	47
γ-$Ga_{0.5}Al_{1.5}O_3$	21	79

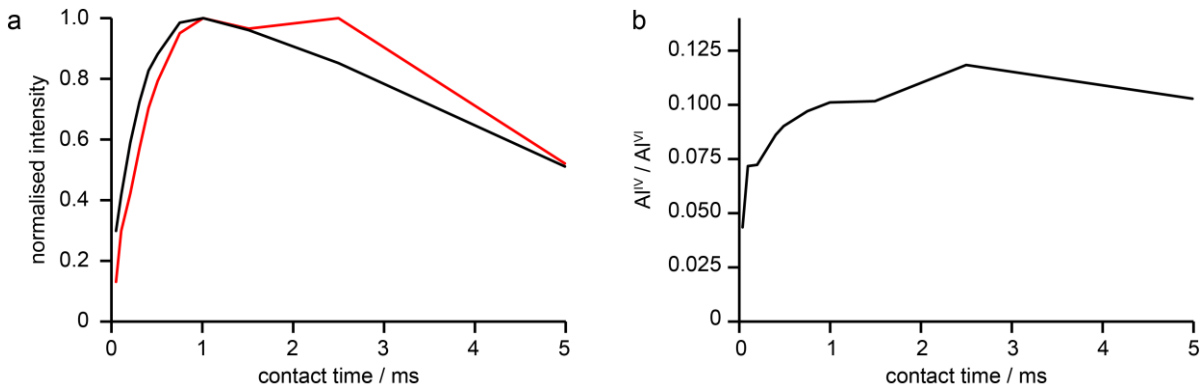

Figure S10: *Plots of (a) integrated intensity of the Al^{IV} (red) and Al^{VI} (black) signals in the ^{27}Al CP MAS NMR spectra of γ-$Ga_{0.5}Al_{1.5}O_3$ as a function of contact time (normalised relative to the maximum intensity for each curve) and (b) the ratio of Al(IV) : Al(VI) as a function of contact time.*

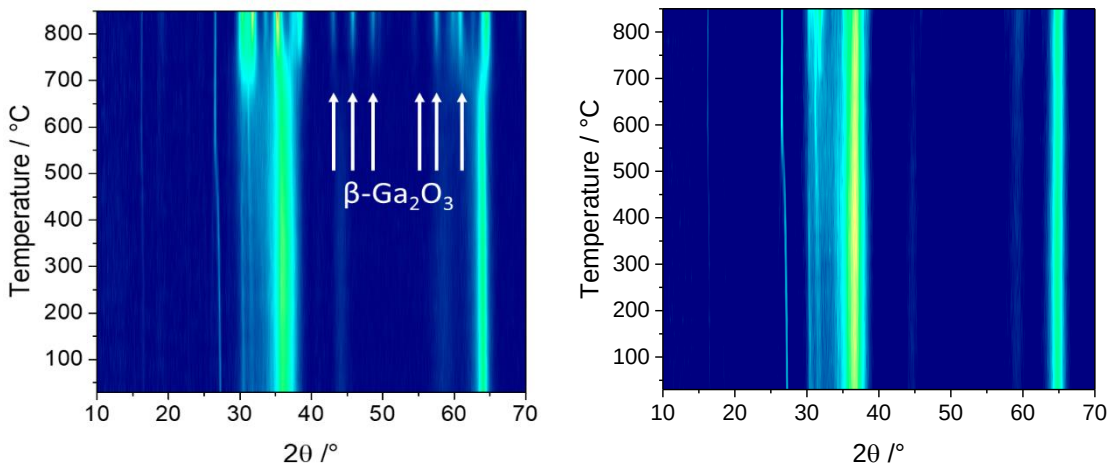

Figure S11: *In situ thermodiffractometry of γ-$Ga_{2-x}Al_xO_3$ spinels (left) x = 0 (right) x = 0.6.*

S4. Additional Data for α-$Ga_{2-x}Al_xO_3$ and β-$Ga_{2-x}Al_xO_3$

Table S7 Refined crystal parameters for β-$Ga_{1.8}Al_{0.2}O_3$ a = 12.17969(16) Å, b = 3.02652(4) Å, c = 5.79034(8) Å, β = 103.8996(11) °, Space group $C2/m$, Rp = 15.1%, wRp = 21.6%

Atom	Wyckoff site	*x*	*y*	*z*	Occupancy	Beq / Å^2
Ga1	4i	0.09020(19)	0	-0.2068(5)	0.923(7)	0.20(11)
Al1	4i	0.09020(19)	0	-0.2068(5)	0.071(7)	0.20(11)
Ga2	4i	0.34139(17)	0	-0.3129(4)	0.871(7)	0.75(13)
Al2	4i	0.34139(17)	0	-0.3129(4)	0.129(7)	0.75(13)
O1	4i	0.1619(7)	0	0.107(2)	1	0.2(3)
O2	4i	0.4963(7)	0	0.2551(12)	1	0.2(3)
O3	4i	0.8277(6)	0	0.425(2)	1	0.3(3)

Table S8 Refined crystal parameters for β-$Ga_{1.4}Al_{0.6}O_3$ a = 12.0711(2) Å, b = 2.99309(5) Å, c = 5.74510(11) Å, β = 103.9722(16) °, Space group $C2/m$, Rp = 13.7%, wRp = 17.7%

Atom	Wyckoff site	*x*	*y*	*z*	Occupancy	Beq / Å^2
Ga1	4i	0.09149(19)	0	-0.2059(4)	0.788(5)	0.77(9)
Al1	4i	0.09149(19)	0	-0.2059(4)	0.212(5)	0.77(9)
Ga2	4i	0.34206(16)	0	-0.3125(4)	0.612(5)	0.6(1)
Al2	4i	0.34206(16)	0	-0.3125(4)	0.388(5)	0.6(1)
O1	4i	0.1607(5)	0	0.1120(16)	1	0.2(19)
O2	4i	0.4971(5)	0	0.2581(9)	1	0.2(19)
O3	4i	0.8273(5)	0	0.4262(17)	1	0.2(19)

Table S9 Refined crystal parameters for β-$Ga_{1.0}Al_{1.0}O_3$ a = 11.99483(11) Å, b = 2.97101(25) Å, c = 5.71499(5) Å, β = 104.0448(7) °, Space group $C2/m$, Rp = 11.1%, wRp = 15.1%

Atom	Wyckoff site	*x*	*y*	*z*	Occupancy	*B*eq / Å^2
Ga1	4i	0.09117(14)	0	-0.2047(3)	0.618(3)	0.54(6)
Al1	4i	0.09117(14)	0	-0.2047(3)	0.382(3)	0.54(6)
Ga2	4i	0.34169(14)	0	-0.3139(3)	0.382(3)	0.52(8)
Al2	4i	0.34169(14)	0	-0.3139(3)	0.618(3)	0.52(8)
O1	4i	0.1623(4)	0	0.108(1)	1	0.2(13)
O2	4i	0.4967(4)	0	0.2570(7)	1	0.2(14)
O3	4i	0.8261(4)	0	0.433(1)	1	0.2(13)

Table S10 Refined crystal parameters for β-$Ga_{0.7}Al_{1.3}O_3$, a = 11.90851(10) Å, b = 2.94608(3) Å, c = 5.67840(5) Å, β = 104.0810(8) °, Space group $C2/m$, Rp = 11.4%, wRp = 15.5%

Atom	Wyckoff site	*x*	*y*	*z*	Occupancy	*B*eq / Å^2
Ga1	4i	0.0907(14)	0	-0.2052(3)	0.463(3)	0.73(7)
Al1	4i	0.0907(14)	0	-0.2052(3)	0.537(3)	0.73(7)
Ga2	4i	0.31483(14)	0	-0.3150(3)	0.237(3)	0.64(8)
Al2	4i	0.31483(14)	0	-0.3150(3)	0.763(3)	0.64(8)
O1	4i	0.1614(3)	0	0.1098(9)	1	0.8
O2	4i	0.4970(4)	0	0.2580(6)	1	0.57(4)
O3	4i	0.8268(3)	0	0.4315(9)	1	0.47(9)

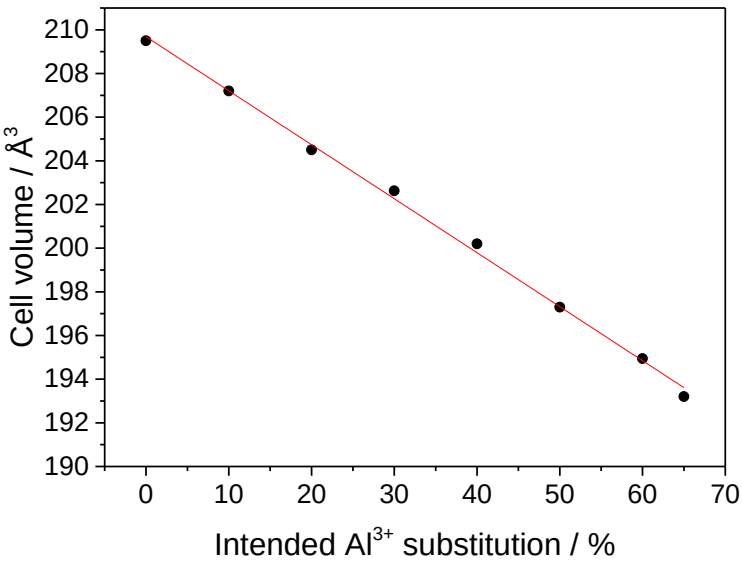

Figure S12: *Plot of cell volume against intended aluminium substitution in β-$Ga_{2-x}Al_xO_3$ showing a linear decrease in accordance with Vegard's law.*

Table S11 Comparison of the changes in tetrahedral and octahedral occupation of Al^{3+} and Ga^{3+} in β-$Ga_{2-x}Al_xO_3$ by Rietveld analysis of powder XRD data and ^{27}Al MAS NMR from samples prepared at 1200 °C and 1400 °C

Sample	**Rietveld**		**^{27}Al NMR**	
	Al^{3+} Occupancy		**Al^{3+} Occupancy**	
	Tet / %	**Oct / %**	**Tet / %**	**Oct / %**
β-$Ga_{1.8}Al_{0.2}O_3$ (1400 °C)	35.8	64.2	30.0	70.0
β-$Ga_{1.6}Al_{0.4}O_3$ (1400 °C)	34.1	65.9	34.6	65.4
β-$Ga_{1.4}Al_{0.6}O_3$ (1200 °C)	35.1	64.9	-	-
β-$Ga_{1.4}Al_{0.6}O_3$ (1400 °C)	35.4	64.6	33.4	66.6
β-$Ga_{1.2}Al_{0.8}O_3$ (1400 °C)	35.9	64.1	38.0	62.0
β-$Ga_{1.0}Al_{1.0}O_3$ (1200 °C)	39.8	60.2	-	-
β-$Ga_{1.0}Al_{1.0}O_3$ (1400 °C)	38.2	61.8	36.9	63.1
β-$Ga_{0.7}Al_{1.3}O_3$ (1400 °C)	41.3	58.7	41.0	59.0

Table S12 Average metal-oxygen bond lengths for the tetrahedral and octahedral sites in β-$Ga_{2-x}Al_xO_3$ with increasing Al^{3+} substitution

Al^{3+} substitution (%)	Tetrahedral average bond length / Å	Octahedral average bond length / Å
0[10]	1.8303	2.0123
10	1.8162	2.0051
30	1.8094	1.9769
50	1.8034	1.9587
65	1.7892	1.9440

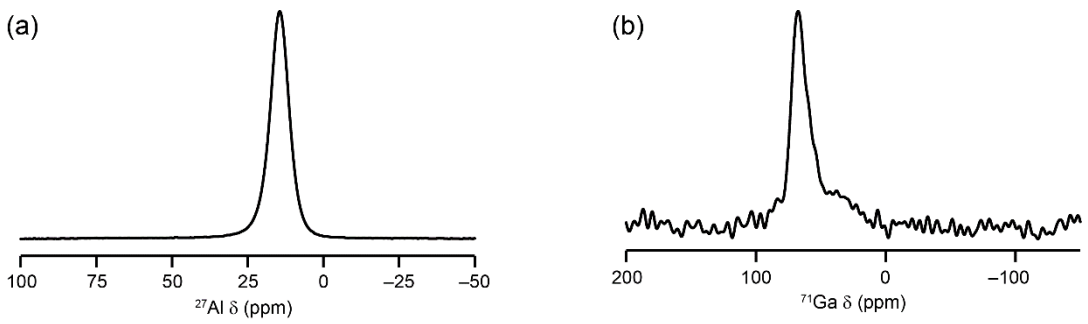

Figure S13: *(a) ^{27}Al (14.1 T, 20 kHz MAS) and (b) ^{71}Ga (20.0 T, 50 kHz MAS) NMR spectra of α-$Ga_{0.2}Al_{1.8}O_3$.*

S5. References

1. Playford, H. Y.; Hannon, A. C.; Barney, E. R.; Walton, R. I., Structures of Uncharacterised Polymorphs of Gallium Oxide from Total Neutron Diffraction. *Chem. Eur. J.* **2013,** *19*, 2803-2813.
2. Yamaguchi, G.; Yanagida, H.; Ono, S., The Crystal Structure of Tohdite. *Bull. Chem. Soc. Jap.* **1964,** *37*, 1555-1557.
3. Pike, K. J.; Malde, R. P.; Ashbrook, S. E.; McManus, J.; Wimperis, S., Multiple-quantum MAS NMR of quadrupolar nuclei. Do five-, seven- and nine-quantum experiments yield higher resolution than the three-quantum experiment? *Sol. State. Nucl. Magn. Reson.* **2000,** *16*, 203-215.
4. Clark, S. J.; Segall, M. D.; Pickard, C. J.; Hasnip, P. J.; Probert, M. J.; Refson, K.; Payne, M. C., First principles methods using CASTEP. *Z. Krist.* **2005,** *220*, 567-570.
5. Pickard, C. J.; Mauri, F., All-electron magnetic response with pseudopotentials: NMR chemical shifts. *Phys. Rev. B* **2001,** *63*, 245101.
6. Perdew, J. P.; Burke, K.; Ernzerhof, M., Generalized gradient approximation made simple. *Phys. Rev. Lett.* **1996,** *77*, 3865-3868.
7. Tkatchenko, A.; Scheffler, M., Accurate Molecular Van Der Waals Interactions from Ground-State Electron Density and Free-Atom Reference Data. *Phys. Rev. Lett.* **2009,** *102*, 073005.
8. Monkhorst, H. J.; Pack, J. D., Special Points For Brillouin-Zone Integrations. *Phys. Rev. B* **1976,** *13*, 5188-5192.
9. Pyykko, P., Year-2017 nuclear quadrupole moments. *Mol. Phys.* **2018,** *116*, 1328-1338.
10. Åhman, J.; Svensson, G.; Albertsson, J., A reinvestigation of β-gallium oxide. *Acta Crystallogr. Sec. C - Cryst. Struct. Commun.* **1996,** *52*, 1336-1338.